ACCOUNTS of chemical research

Article

pubs.acs.org/accounts

Surface-Catalyzed C−C Covalent Coupling Strategies toward the Synthesis of Low-Dimensional Carbon-Based Nanostructures

Published as part of the Accounts of Chemical Research special issue "Microscopic Insights into Surface Catalyzed Chemical Reactions".

Qitang Fan,[†] J. Michael Gottfried,[‡] and Junfa Zhu*[,†]

[†]National Synchrotron Radiation Laboratory and Collaborative Innovation Center of Suzhou Nano Science and Technology, University of Science and Technology of China, Hefei 230029, People's Republic of China

[‡]Fachbereich Chemie, Philipps-Universität Marburg, Hans-Meerwein-Strasse 4, 35032 Marburg, Germany

CONSPECTUS: Carbon-based nanostructures have attracted tremendous interest because of their versatile and tunable properties, which depend on the bonding type of the constituting carbon atoms. Graphene, as the most prominent representative of the π-conjugated carbon-based materials, consists entirely of sp^2-hybridized carbon atoms and exhibits a zero band gap. Recently, countless efforts were made to open and tune the band gap of graphene for its applications in semiconductor devices. One promising method is periodic perforation, resulting in a graphene nanomesh (GNM), which opens the band gap while maintaining the exceptional transport properties. However, the typically employed lithographic approach for graphene perforation is difficult to control at the atomic level. The complementary bottom-up method using surface-assisted carbon−carbon (C−C) covalent coupling between organic molecules has opened up new possibilities for atomically precise fabrication of conjugated nanostructures like GNM and graphene nanoribbons (GNR), although with limited maturity. A general drawback of the bottom-up approach is that the desired structure usually does not represent the global thermodynamic minimum. It is therefore impossible to improve the long-range order by postannealing, because once the C−C bond formation becomes reversible, graphene as the thermodynamically most stable structure will be formed. This means that only carefully chosen precursors and reaction conditions can lead to the desired (non-graphene) material.

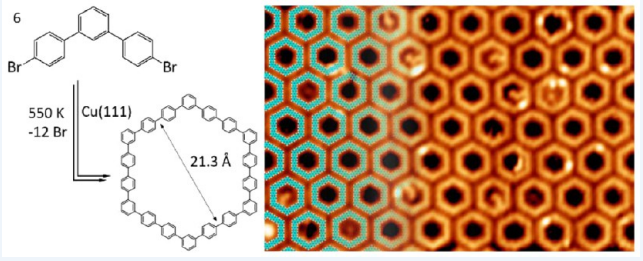

One of the most popular and frequently used organic reactions for on-surface C−C coupling is the Ullmann reaction of aromatic halides. While experimentally simple to perform, the irreversibility of the C−C bond formation makes it a challenge to obtain long-range ordered nanostructures. With no postreaction structural improvement possible, the assembly process must be optimized to result in defect-free nanostructures during the initial reaction, requiring complete reaction of the precursors in the right positions. Incomplete connections typically result when mobile precursor monomers are blocked from reaching unsaturated reaction sites of the preformed nanostructures. For example, monomers may not be able to reach a randomly formed internal cavity of a two-dimensional (2D) nanostructure island due to steric hindrance in 2D confinement, leaving reaction sites in the internal cavity unsaturated. Wrong connections between precursor monomers, here defined as intermolecular C−C bonds forcing the monomer into a nonideal position within the structure, are usually irreversible and can induce further structural defects. The relative conformational flexibility of the monomer backbones permits connections between deformed monomers when they encounter strong steric hindrance. This, however, usually leads to heterogeneous structural motifs in the formed nanostructures.

This Account reviews some of the latest developments regarding on-surface C−C coupling strategies toward the synthesis of carbon-based nanostructures by addressing the above-mentioned issues. The strategies include Ullmann coupling and other, "cleaner" alternative C−C coupling reactions like Glaser coupling, cyclo-dehydrogenation, and dehydrogenative coupling. The choice of substrate materials and precursor designs is crucial for optimizing substrate reactivity and precursor diffusion rates, and to reduce events of wrong linkage. Hierarchical polymerization is employed to steer the coupling route, which effectively improves the completeness of the reaction. Effects of byproducts on nanostructure formation is comprehended with both experimental and theoretical studies.

INTRODUCTION

Low-dimensional nanostructured materials exhibit unprecedented dimension-related properties compared with their bulk counterparts. Especially carbon-based materials have received

Received: March 30, 2015
Published: July 21, 2015

DOI: 10.1021/acs.accounts.5b00168
Acc. Chem. Res. 2015, 48, 2484−2494

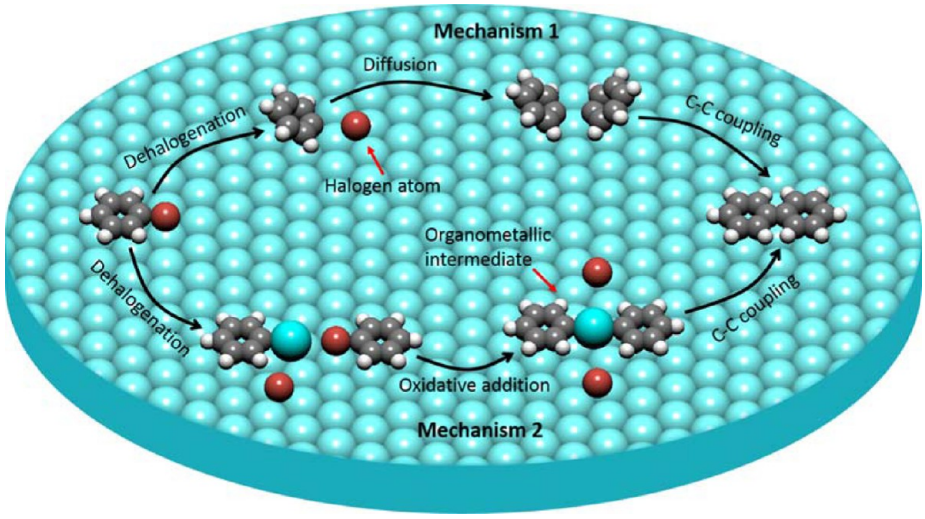

Figure 1. Two reaction mechanisms of the surface-assisted Ullmann reaction. Gray, white, red, and cyan spheres represent carbon, hydrogen, halogen, and metal atoms, respectively.

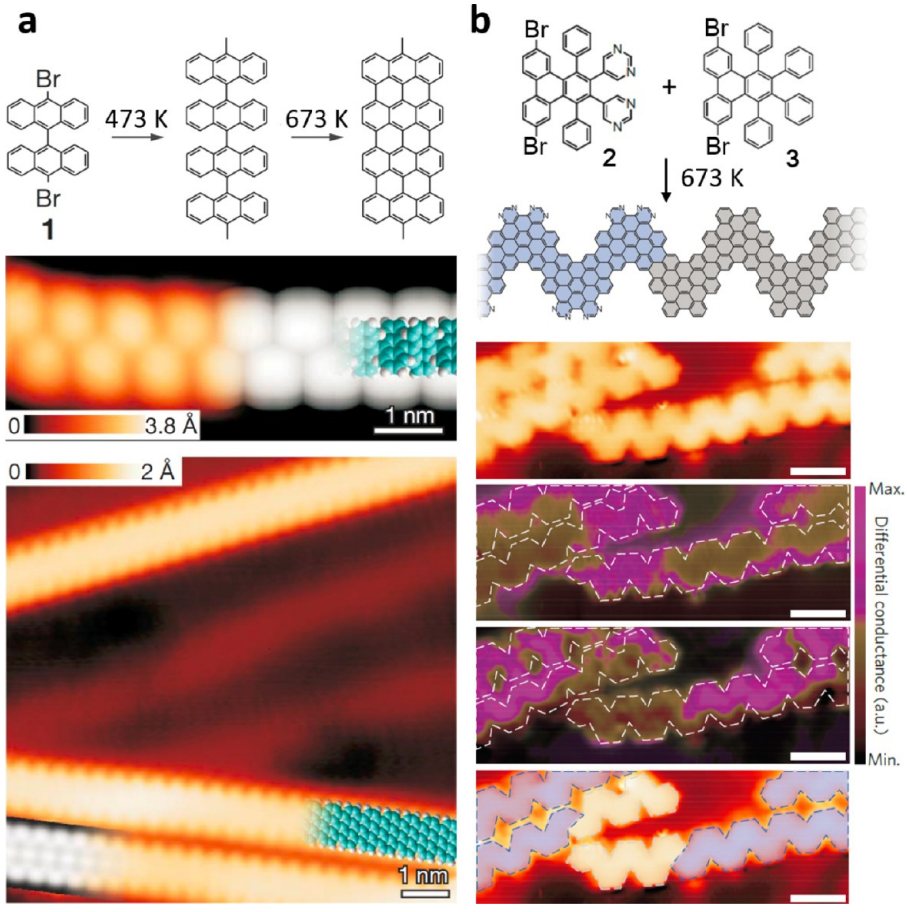

Figure 2. (a) Formation of graphene nanoribbons (GNR) on Au(111) by Ullmann coupling of monomer **1** followed by cyclo-dehydrogenation. The experimental STM images of polyanthrylene (with varied contrast) evolve into GNRs (with uniform contrast) after annealing at 400 K. (b) p-N-GNR heterostructures obtained from **2** and **3**. The varied contrast in the experimental STM image of p-N-GNR and the corresponding differential dI/dV map indicate the existence of heterojunctions in p-N-GNRs. Reproduced with permission from refs 9 and 28. Copyright 2010 and 2014 Nature Publishing Group.

tremendous attention due to their lightness, versatility, and low costs. Graphene, as a rapidly rising star among low-dimensional carbon-based materials, features long-range π-conjugation and zero band gap, which result in remarkable in-plane carrier transport properties[1] and make graphene a promising candidate for usage in electronic devices. However, the zero band gap property of graphene also limits its application in some semiconductor devices like field-effect transistors. Theory predicts that a band gap can be induced by forming an antidot lattice on graphene by periodic perforation.[2] Furthermore, the

DOI: 10.1021/acs.accounts.5b00168
Acc. Chem. Res. 2015, 48, 2484−2494

band gap can be tuned via the antidot lattice parameters.[3] Experimentally, 20−400 nm holes were obtained by lithography.[4−7] Nevertheless, atomic-level control of the hole structure cannot be achieved using these top-down lithographic methods.

Alternatively, covalently bonded organic frameworks (COFs), including graphene derivatives, are available by on-surface bottom-up synthetic approaches, which promise more control over the local structure. So far, graphene-related nanostructures like porous graphene,[8] graphene nanoribbons (GNR),[9−11] and nanographenes[12] have been synthesized by surface-assisted C−C coupling of molecular aromatic precursors. Their electronic properties are typically characterized by a small bandgap: An example is the reported 1.6 eV bandgap for arm-chaired GNR; this bandgap is reduced with increasing width of the GNR.[9] In principle, structures and properties of the networks can be steered by careful design and functionalization of the precursor structures. Nevertheless, controlling the C−C coupling process such that structurally homogeneous, long-range ordered networks are obtained remains a challenge. Uniformity of product structures and the absence of secondary reactions have made the Ullmann reaction of aromatic halides popular for on-surface C−C coupling in ultrahigh vacuum (UHV). High-quality 1D-GNR[9] and poly(*para*-phenylene)[13] were obtained by Ullmann coupling of 2-fold halogenated monomers. However, 2D networks obtained from monomers with three or more halogen substituents were typically characterized by small branched domains and structural heterogeneity. The main problem is that initially formed defects cannot heal, because the reaction is performed under conditions where the C−C bond formation is nonreversible. (Otherwise graphene as the thermodynamically favored product would be obtained.) Efforts were made to address this problem by careful selection of reaction conditions, monomer structure, and substrate. Combined scanning tunneling microscopy (STM) experiments and Monte Carlo simulations demonstrated that the compactness of the formed networks could be optimized by steering monomer diffusion and coupling rates.[14,15] Long-range order and compactness of the networks can also be improved by hierarchical coupling strategies: In the first step, the monomers form larger molecules, which are coupled to form a network in a second step. The two-step approach, which requires monomers with sites of different reactivity, was shown to reduce the amount of internal cavities in network domains.[14,16]

The halogen atoms released during the Ullmann coupling represent another factor that undermines the long-range order of the network.[17] They aggregate into islands, which compete with the already formed network domains and inhibit their further growth. To avoid these adverse effects, "clean" C−C coupling reactions such as Glaser coupling,[18] Bergman cyclization,[19] cyclo-dehydrogenation,[12,20] and dehydrogenative coupling[21,22] have been proposed. However, these reactions have their own disadvantages such as multiple reaction pathways during Glaser coupling, simultaneous isomerization of monomers during Bergman cyclization and strong substrate-dependence for C−H dehydrogenative coupling. This Account outlines the recently developed surface-assisted C−C coupling strategies for the fabrication of low-dimensional carbon-based nanostructures. By comparing their characteristics, possible optimizations of the experimental conditions are proposed, aiming at the synthesis of nanostructures with larger domains and improved long-range order.

SURFACE-ASSISTED ULLMANN COUPLING

The Ullmann reaction was originally developed as a C−C coupling between aromatic halides induced by copper (which

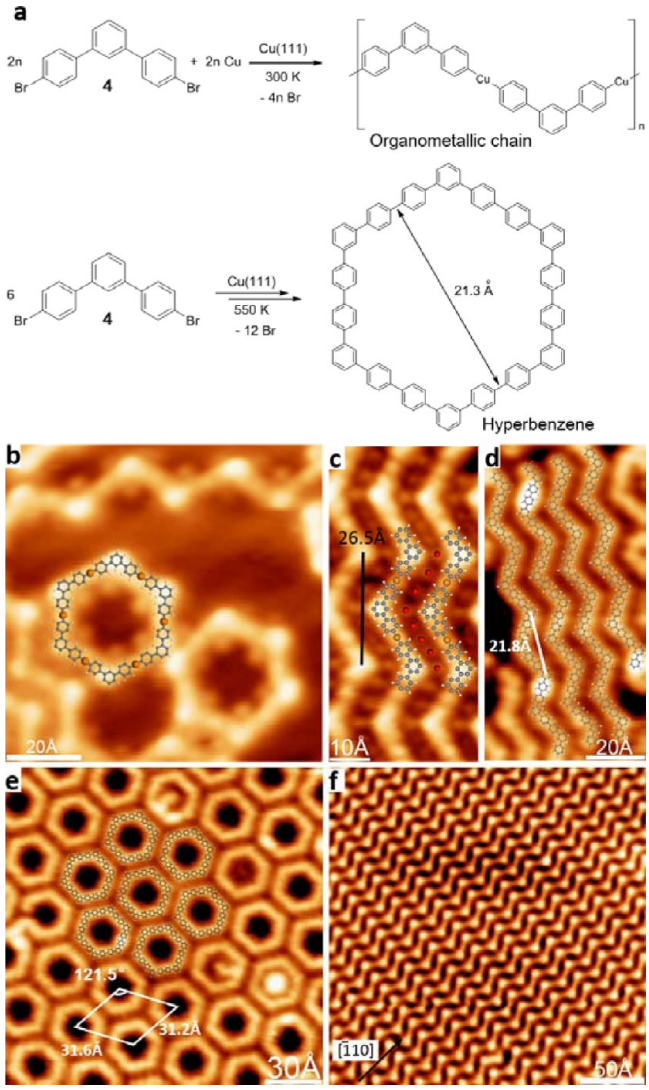

Figure 3. (a) Surface-assisted Ullmann reaction of 4,4″-dibromo-*m*-terphenyl (DMTP, **4**) forming organometallic chains at 300 K and hyperbenzene molecules at 550 K on Cu(111). STM images of (b) organometallic chain and hexamer obtained by deposition of DMTP onto Cu(111) at 300 K, (c) organometallic chains superimposed with molecular model, (d, e) oligophenylene chains and hyperbenzene arrays obtained after deposition of DMTP onto Cu(111) held at 550 K and (f) defect-free organometallic chain domain prepared by deposition of DMTP onto Cu(111) at 440 K. Reproduced with permission from refs 31 and 32. Copyright 2013 Wiley-VCH and Copyright 2014 American Chemical Society.

reacts to the corresponding Cu halide).[23] It has recently been transferred to solid surfaces (mostly coinage metals) in UHV for on-surface synthesis of 1D and 2D polymers. The reaction mechanism may be substrate- and molecule-dependent, also because the necessary reaction conditions vary with the substrate.[24] Figure 1 shows two typical mechanisms, which differ in the presence[25] or absence[26] of organometallic intermediates as proposed by previous works. One of the first applications was the coupling of tetraphenylporphyrins (TPP) with different numbers and positions of peripheral Br atoms

DOI: 10.1021/acs.accounts.5b00168
Acc. Chem. Res. 2015, 48, 2484−2494

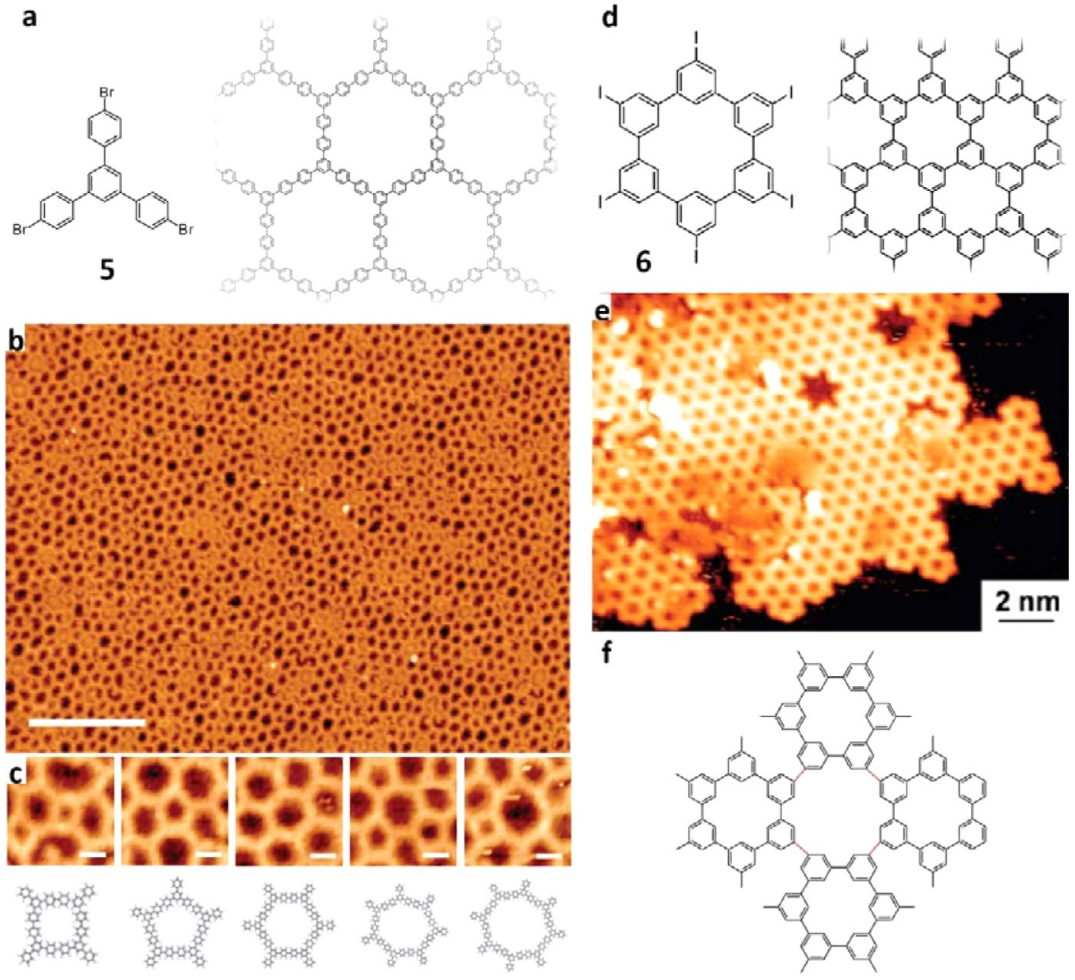

Figure 4. (a, d) Chemical structure of 1,3,5-tris(4-bromophenyl)benzene (TBPB, **5**), hexaiodo-substituted cyclohexa-*m*-phenylene (CHP, **6**), and the 2D polyphenylene networks based on TBPB and CHP. STM images of (b) extended nanoporous covalent network composed predominantly of (c) polygons with four, five, six, seven, and eight edges and (e) 2D polyphenylene superhoneycomb network on Ag(111) formed after polymerization of CHP at 805 K. (f) Chemical structure of a proposed octagon consisting of four CHPs. Scale bars in panels b and c are 150 and 14 Å, respectively. Reproduced with permission from refs 15 and 35. Copyright 2010 American Chemical Society and Copyright 2010 the Royal Society of Chemistry.

resulting in the formation of dimers, chains, and 2D arrays on Au(111).[27] Since no organometallic intermediates were observed, the reaction possibly followed mechanism **1**.

More recently, straight and chevron-type GNRs were obtained on Au(111) from precursors like 10,10′-dibromo-9,9′-bianthryl (**1**, DBPM), 5,5-(6,11-dibromo-1,4-diphenyltriphenylene-2,3-diyl)dipyrimidine (**2**), and 6,11-dibromo-1,2,3,4-tetraphenyl-triphenylene (**3**) by Ullmann coupling at 473 K and subsequent cyclo-dehydrogenation at 673 K.[9,28] While monomer **1** resulted in straight GNRs (Figure 2a),[9] chevron-type GNR heterostructures with segments of pristine graphene nanoribbons (p-GNRs) and nitrogen-doped graphene nanoribbons (N-GNRs) were obtained from monomers **2** and **3** (Figure 2b).[28] The different sections were distinguished in STM by variation of contrast and differential conductance (dI/dV) maps. These heterostructures behaved similarly to traditional p−n junctions and thus may find applications in photovoltaics and electronics. Various other 1D polymers were obtained by Ullmann coupling on copper and silver surfaces.[13,29,30] Unlike on Au, organometallic intermediates were commonly observed, in line with mechanism **2** in Figure 1.

The Ullmann coupling is also useful for the on-surface synthesis of large molecules, which are not available by solution-based synthesis or are too large for vapor deposition. Using 4,4″-dibromo-*meta*-terphenyl (DMTP, **4**), a cyclic hexagonal oligophenylene consisting of 18 phenyl rings (hyperbenzene) was synthesized on Cu(111) (Figure 3).[31] Deposition of **4** at 550 K resulted in the direct formation of the hydrocarbon macrocycle (Figure 3a,e) with some oligophenylene chains as side products (Figure 3d). In contrast, organometallic intermediates with C−Cu−C bonds occurred after deposition at 300 K. Besides the organometallic macrocycles in Figure 3b, which represent direct intermediates to the hyperbenzene macrocycles, chains were observed, which formed large islands held together by Br adatoms (Figure 3c,f).[32] Related observations were made for $(\text{anthryl-Ag})_n$ Ag(111)-supported organometallic chains, which were stabilized by Br atoms through Br···H hydrogen bonds.[33] C−C coupling was typically monitored by local probe measurements, observing the shrinking compared with organometallic intermediates, but also with chemically sensitive techniques like fast X-ray photoelectron spectroscopy (fast-XPS) and near-

DOI: 10.1021/acs.accounts.5b00168
Acc. Chem. Res. 2015, 48, 2484−2494

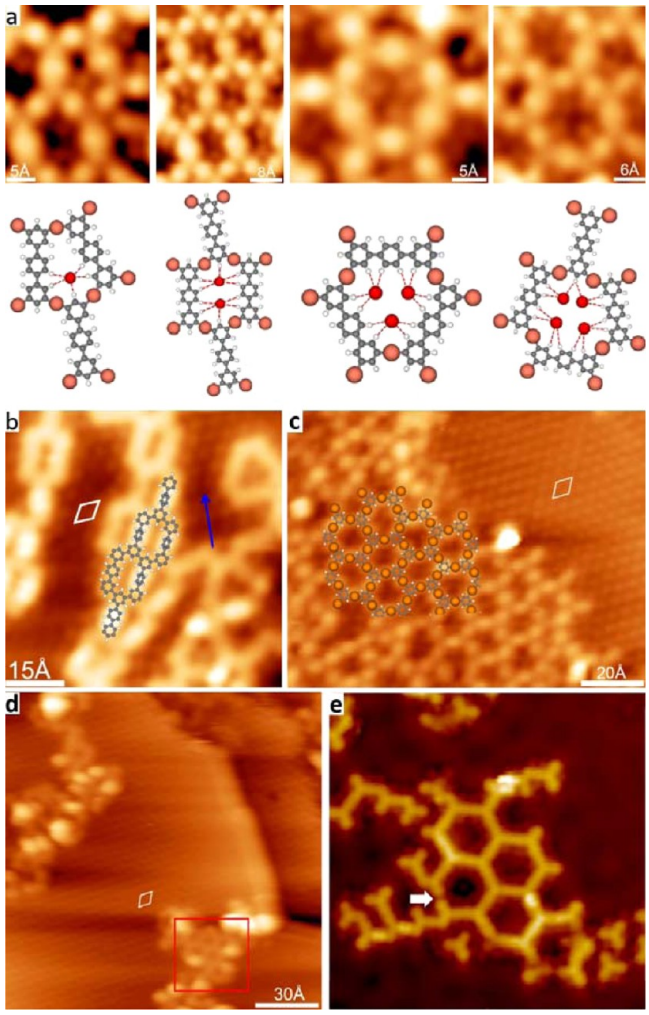

Figure 5. STM images of (a) organometallic nanopores enclosing one, two, three, and four Br atoms with molecular model underneath, based on 3,5,3″,5″-tetrabromo-*para*-terphenyl (TBrTP) on Cu(111), (b) covalent networks (overlaid with molecular model) formed by C−C coupling of TBrTP on Cu(111) held at 570 K, (c) organometallic networks obtained after deposition of TriBB onto Cu(111) held at 420 K, (d) covalent networks obtained by annealing the sample in panel c to 520 K, and (e) covalent networks formed by C−C coupling of TBPB on Cu(111) surface at 473 K. Reproduced with permission from refs 17, 37, and 38. Copyright 2014 American Chemical Society, Copyright 2015 American Institute of Physics, and Copyright 2014 American Chemical Society.

edge X-ray absorption fine structure spectroscopy (NEXAFS).[34]

Compared with 1D polymers, 2D polymers are much more difficult to synthesize with satisfactory long-range order. The Ullmann reaction requires monomers with three or more halogen substituents such as 1,3,5-tris(4-bromophenyl)benzene (TBPB, **5**), which was used with the aim to prepare a 2D polymer with hexagonal pores on Au(111) (Figure 4a).[35] However, the resulting network was composed of various different polygons with four, five, six, seven, or eight edges (Figure 4c) because of the conformational flexibility of the TBPB skeleton, which allows the deformation of precursor monomers with limited tension.[36] Possibly, using a precursor monomer with enhanced structural rigidity would result in a more uniform network.

Hexaiodo-substituted cyclohexa-*m*-phenylene (CHP, **6**; Figure 4d) was used to fabricate 2D polyphenylene networks on Cu(111), Ag(111), and Au(111).[15] This macrocycle is stiffer than TBPB since the six phenyl units are interlinked. Therefore, unwanted polygons such as the octagons (Figure 4f) have scarcely been observed in network domains. Even though the compactness of the acquired 2D polyphenylene networks varied with the coupling probability influenced by different substrates, the defects in the network were only regular cavities, as shown by the star-shaped holes in the network (Figure 4e). Internal cavities and wrong polygons in the network can be considered as incompleteness of the coupling reactions and the formation of wrong connections, respectively. The completeness can be improved via sequential precursor monomer dosing and coupling reaction. For example, the star-shaped cavity defects can be repaired by coupling with one additional precursor molecule in a second deposition process. However, the wrong connections cannot be remedied due to the irreversibility of the C−C bond formation.

For fabricating long-range ordered 2D polymers, it is important to avoid deformation of monomers during the C−C coupling process. Such deformation can be induced by neighboring molecules or atoms on the surface. For the Ullmann reaction, it has been shown that the Br adatoms can pose significant steric hindrance to the formation of both organometallic and C−C covalent bonded networks. The deposition of 3,5,3″,5″-tetrabromo-*para*-terphenyl (TBrTP) onto Cu(111) at 300 K led to organometallic networks with nanopores of different sizes.[17] Depending on the pore sizes, between one and four Br atoms were enclosed (Figure 5a). Statistical analysis showed that the number of enclosed Br atoms was directly correlated to the pore size, suggesting that the steric hindrance exerted by Br defined the pore size.

Higher substrate temperatures of 570 K during TBrTP deposition resulted in C−C bonded networks, as shown in Figure 5b. The Br adatoms were found in close-packed islands (blue arrow) with a $(\sqrt{3} \times \sqrt{3})R30°$ structure (marked with white hexagonal unit cell). These Br islands surrounded the network domain, inhibiting the further coupling of TBrTP monomers to this domain. As expected, this problem was aggravated with increasing number of Br atoms per precursor molecule: Organometallic networks obtained from 1,3,5-tribromo-benzene (TriBB) on Cu(111) surface (Figure 5c) can only cover ∼60% of the surface, because the rest is occupied by Br atoms in network nanopores and Br islands.[37] Annealing this sample to 520 K gave rise to the formation of covalent networks (red framed in Figure 5d), which occupied an even smaller proportion (∼30%) of the surface area. The remaining ∼70% of the surface was covered by Br islands. Figure 5e shows a section of a 2D polymer network with larger pore size obtained by C−C coupling of TBPB on Cu(111).[38] The incomplete edge marked by the whited arrow may stem from the steric hindrance exerted by Br atoms inside the hexagon. This analysis sheds light on design criteria for monomers yielding large-area 2D polymers: For halogen-substituted aromatics, the dimensions of the carbon skeleton should be large enough to form pores that can enclose at least the stoichiometric number of the halogen atoms that occur as byproduct. Only then the growth of a porous 2D polymer can possibly extend over the whole surface area.

DOI: 10.1021/acs.accounts.5b00168
Acc. Chem. Res. 2015, 48, 2484−2494

SURFACE-ASSISTED HALOGEN-FREE COUPLING STRATEGIES

The halogen atoms released during the Ullmann reaction represent a major problem, because they can interfere with the formation of long-range ordered structure and often cannot be desorbed after the reaction without destroying the organic polymer. To overcome this problem, surface-assisted clean coupling strategies have been proposed, in which byproducts desorbed from the surface during the reaction. One example for a "clean" on-surface coupling is the "Glaser coupling" of alkynes with desorption of the byproduct H_2 (Figure 6a). Gao et al. studied this reaction using two arylalkynes (**7** and **8**) with alkyl side groups and different dimensions (Figure 6b).[18] It has been shown that **7** and **8** undergo oligomerization through homocoupling, trimerization, or other reactions on Au(111) after annealing at 396–413 K. However, homocoupling between terminal alkynes, yielding linear oligomers, was more efficient and selective on Ag(111) than Au(111) as shown by the longer linear oligomers with increased yield in Figure 6e,f compared with Figure 6c,d, respectively. Besides the substrate, the precursor structure can affect the reaction pathway. Alkyne **8** had a shorter reacting alkyne moiety, thus the *ortho*-positioned alkyl substituents were found to largely suppress side reactions and favor homocoupling for steric reasons. As shown in Figure 6d,f, linear polymer chains obtained from **8** maintained higher degrees of order compared with oligomers obtained from **7** on both Au(111) and Ag(111) surfaces (Figure 6c,e).

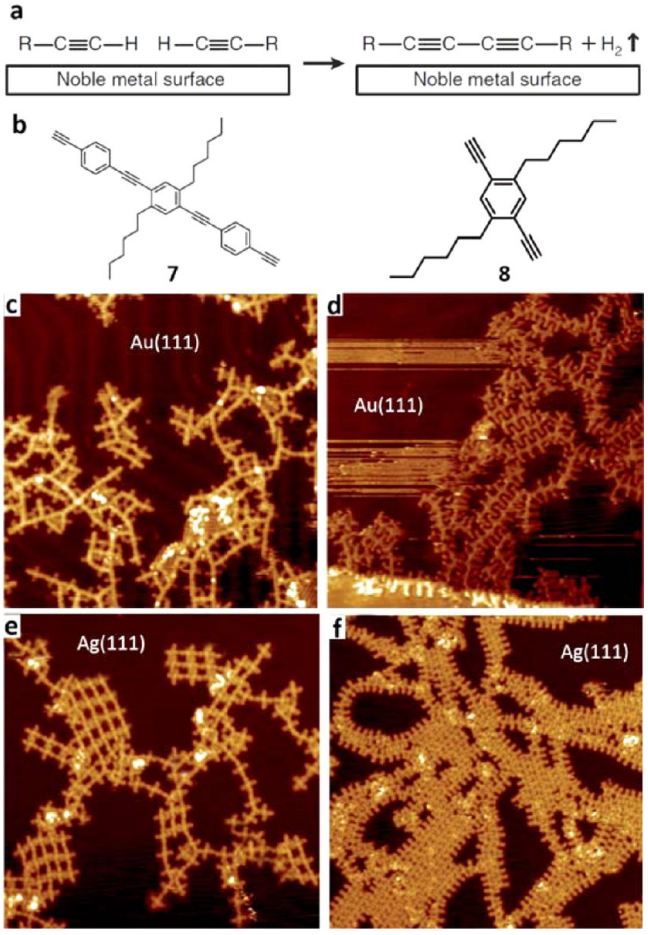

Figure 6. (a) Surface-assisted homocoupling reaction of alkynes. (b) Chemical structure of two alkynes, **7** and **8**. STM images of (c, e) oligomers formed from alkyne **7** on Au(111) and Ag(111) after annealing at 396–413 K (40 × 40 nm^2) and (d, f) 1D polymer chains formed from alkyne **8** on Au(111) and Ag(111) after annealing (25 × 25 and 40 × 40 nm^2). Reproduced with permission from ref 18. Copyright 2013 Wiley-VCH.

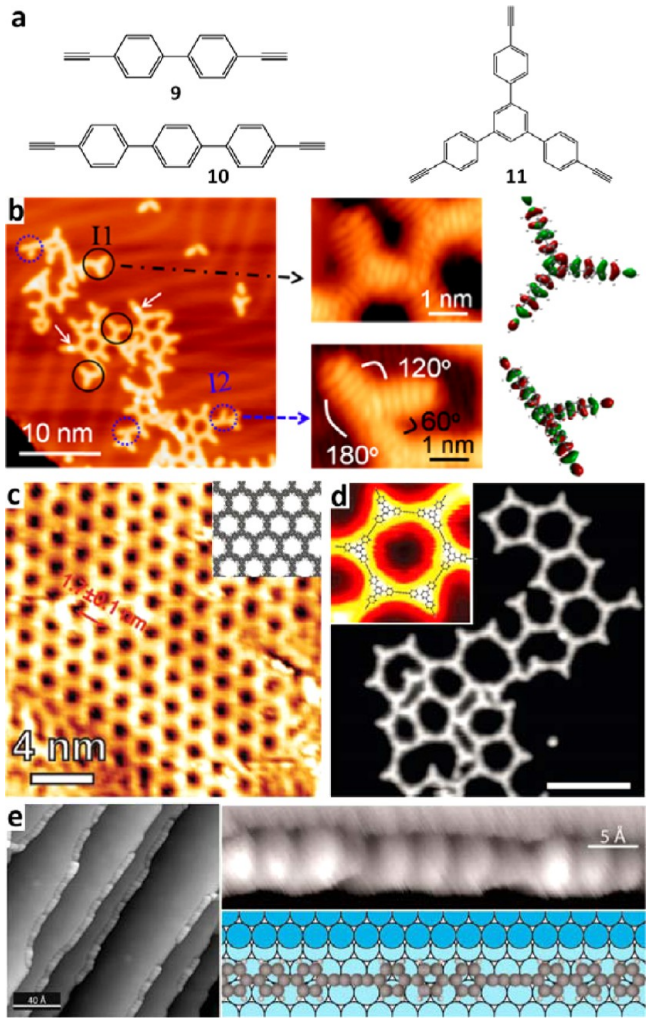

Figure 7. (a) Chemical structures of 4,4′-diethynyl-1,1′-biphenyl (**9**, DEBP), 4,4″-diethynyl-1,1′:4′,1″-terphenyl (DETP, **10**), and 1,3,5-tris(4-ethynylphenyl)benzene (TEB, **11**). STM images of (b) networks obtained by DEBP polymerization on Au(111) at 373 K and two types of molecular interconnections with molecular orbitals given alongside, (c) a regular domain of 2D polymer network (molecular model in inset) obtained by cyclotrimerization of TEB on Au(111) at 433 K, (d) covalent network patches formed through annealing TEB on Ag(111) to 400 K (calculated model in inset), and (e) extended-graphdiyne wires (with magnified view and molecular model) formed by annealing DETP on Ag(877) at 450 K. Reproduced with permission from refs 39–42. Copyright 2014 American Chemical Society, Copyright 2014 the Royal Society of Chemistry, Copyright 2012 Nature Publishing Group, and Copyright 2014 American Chemical Society.

Au(111) was shown to favor the cyclotrimerization of alkynes, such as 4,4′-diethynyl-1,1′-biphenyl (DEBP, **9**) and 1,3,5-tris(4-ethynylphenyl)benzene (TEB, **11**) (Figure 7a). Cyclotrimerization of **9** on Au(111) at 373 K gave rise to structures with branched and hexagonal motifs with two types of molecular interconnections, I1 and I2 (Figure 7b).[39] The more uniform polyphenylene structure in Figure 7c (molecular

DOI: 10.1021/acs.accounts.5b00168
Acc. Chem. Res. 2015, 48, 2484–2494

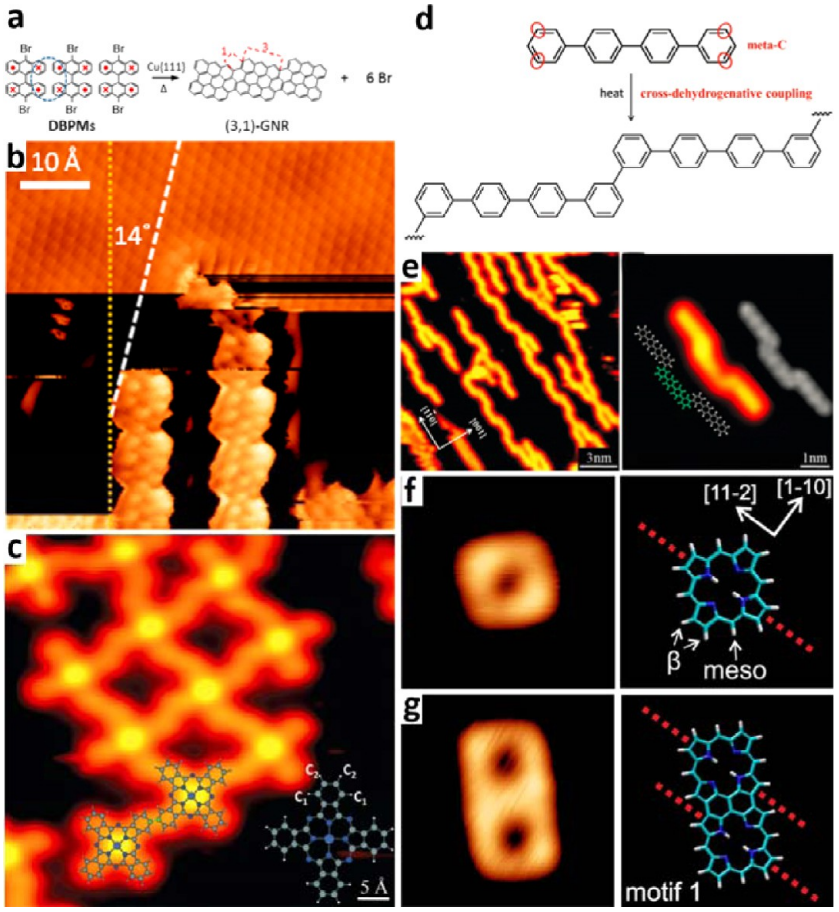

Figure 8. Reaction schemes for (a) polymerization of DBPM **1** into (3,1)-GNR and (d) cross-dehydrogenation coupling of quaterphenyl (4Ph) molecules into polyphenylene chains. STM images of (b) (3,1)-GNR obtained by annealing DBPM on Cu(111) at 773 K, (c) 2D polymer structure formed by annealing the CoPc covered Ag(110) at ~680 K, (e) polyphenylene chains obtained after annealing 4Ph on Cu(110) at 500 K and oligophenylene chain with molecular model (right), (f) single 2H-porphin (2HP) molecule, and (g) 2HP dimer obtained by C−C coupling of 2HP on Ag(111) at 573 K with molecular model. Reproduced with permission from refs 20, 22, 44, and 45. Copyright 2014 American Chemical Society, Copyright 2014 Royal Society of Chemistry, Copyright 2015 Royal Society of Chemistry, and Copyright 2014 American Chemical Society.

model in inset) can be obtained by cyclotrimerization of **11** on Au(111), which is proven by its pore-to-pore distance of 1.7 ± 0.1 nm.[40] On Ag(111), **11** favored the homocoupling reaction pathway in line with related observation described above (see ref 18).[41] As shown in Figure 7d, irregular open-porous networks were obtained after annealing **11** on Ag(111). The fact that not only pores with the ideal hexagonal shape were formed can again be attributed to the flexibility of the monomer backbones and the resulting distortion. The coupling of the linear 4,4″-diethynyl-1,1′:4′,1″ terphenyl (DETP, **10**) on Ag(111) led to irregularly branched networks due to thermally activated side reactions.[42] In contrast, alignment of **10** at the step edges of a Ag(877) surface resulted in linear homocoupling, permitting the controlled synthesis of extended graphydyne wires (Figure 7e). In summary, synthesis of large-scale high-quality 2D conjugated polymers with alkyne monomers still requires an elaborate selection of substrate and precursor monomers to avoid side reactions and distortion of molecular backbones.

Another promising clean coupling strategy is the arene−arene coupling via the oxidative reaction of sp^2 C−H/sp^2 C−H bonds. The crucial issue of this reaction type, to ensure sufficient selectivity, can be overcome, as was demonstrated by the selective C−H activation and dehydrogenative C−C coupling of linear alkanes on Au(110).[43] Another example is the intramolecular cyclo-dehydrogenation between aryl groups.[9,10,12] Recently, it has been shown that the intermolecular aryl−aryl coupling via C−H activation has a huge potential for the fabrication of clean 1D and 2D polymers from aromatic precursors. Han et al. reported surprising results for the polymerization of 10,10′-dibromo-9,9′-bianthryl (**1**, DBPM) on Cu(111).[20] Unlike the straight GNRs formed on Au(111), the Ullmann C−C coupling at the brominated sites of DBPM failed to happen on the Cu(111) surface. Instead, cyclo-dehydrogenation between neighboring DBPM molecules (marked by blue dashed oval in Figure 8a) occurred, resulting in a zigzagged (3,1)-GNR (Figure 8b). It was postulated that intact DBPM assembles into chains through $\pi-\pi$ stacking, prepositioning DBPM into configurations favoring polymerization through cyclo-dehydrogenation rather than Ullmann coupling.

Sun et al. reported selective aryl−aryl coupling between tetraphenyl (4Ph) molecules on Cu(110).[22] It was proposed that the four equivalent C−H bonds (red ovals in Figure 8d) can be activated selectively by annealing at 500 K, resulting in the formation of tortuous polyphenylene chains (Figure 8e). Two-dimensional polymers based on cobalt−phthalocyanine (CoPc) were obtained on Ag(110) by aryl−aryl coupling at the eight equivalent C_2 sites (Figure 8c).[44] Activation of peripheral C−H bonds was also observed for 2H-porphin (2HP) on

DOI: 10.1021/acs.accounts.5b00168
Acc. Chem. Res. 2015, 48, 2484−2494

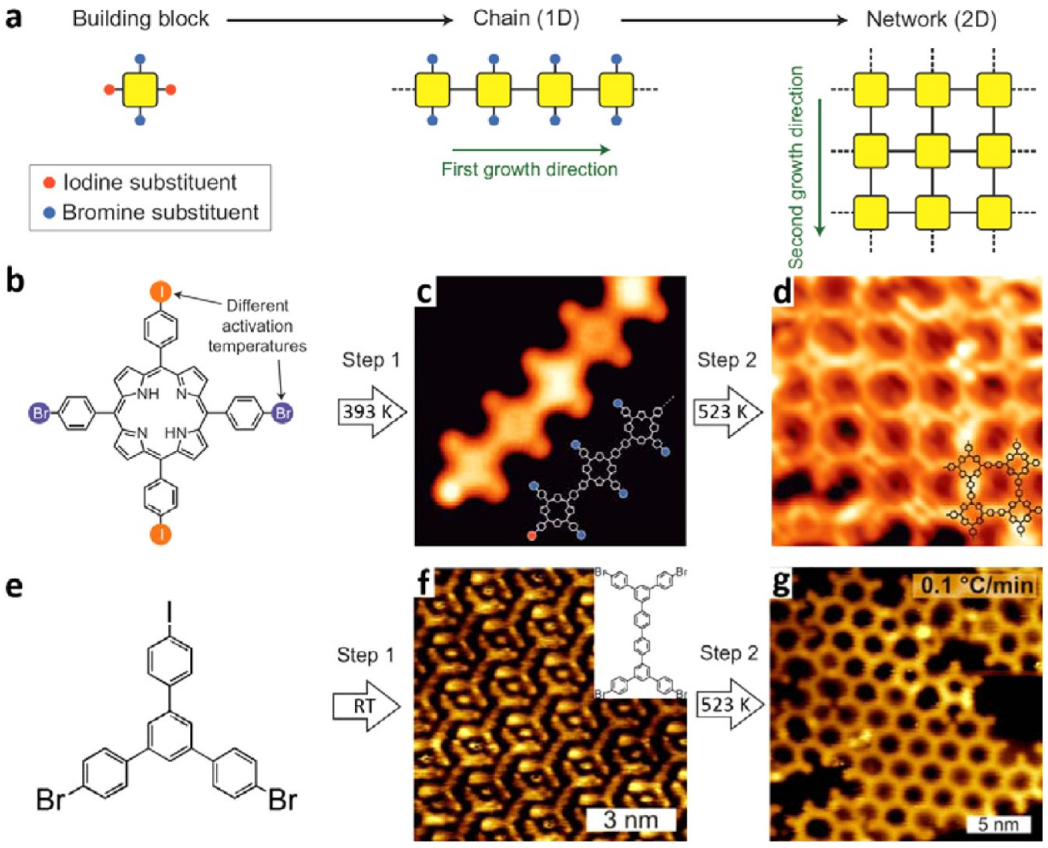

Figure 9. (a) Scheme of a hierarchical coupling strategy. Chemical structures of (b) 5,15-bis(4′-bromophenyl)-10,20-bis(4′-iodophenyl)porphyrin (*trans*-Br_2I_2TPP) and (e) 1,3-bis(*para*-bromophenyl)-5-(*para*-iodophenyl)benzene (BIB). STM images of (c, d) *trans*-Br_2I_2TPP molecules on Au(111) after deposition at 80 K followed by heating to 393 K (step 1) and 523 K (step 2), and (f, g) BIB on Au(111) after deposition at room temperature (step 1) and annealing to 523 K (step 2). Reproduced with permission from refs 14 and 16. Copyright 2014 American Chemical Society and Copyright 2012 Nature Publishing Group.

Ag(111): Figure 8f shows the STM image of an intact single 2HP molecule. Annealing at 573 K led to dehydrogenative coupling into a porphin dimer (Figure 8g) and other oligomers.[45] However, different binding motifs between porphins were observed due to the simultaneous activation of different C−H bonds.

■ OPTIMIZATION OF C−C COUPLING STRATEGIES

After reviewing various C−C coupling strategies, we will now discuss optimized experimental conditions for the synthesis of well-ordered nanostructures. As two major issues causing vacancies and heterogeneous structural motifs in 2D nanostructures, we identified incompleteness of reactions and wrong C−C connections between building blocks. The reaction completeness depends on the coupling probability $p = \nu_{coupl}/(\nu_{coupl} + \nu_{diff})$ with ν_{coupl} and ν_{diff} denoting coupling and diffusion rates. Low p values correspond to high surface mobility of building blocks and their enhanced incorporation probability into more compacted networks.[15] However, even at low p values, vacancy defects persist in the network because precursor molecules are hindered from diffusing across domain boundaries. This can be compensated by sequential precursor deposition, because the subsequently dosed precursors can fill the vacancies.

Another effective method to improve the quality and compactness of 2D networks is hierarchical coupling. Grill et al. proposed a hierarchical reaction route for the C−C coupling by selective and sequential activation of C−X sites with different halogen substituents X, as shown in Figure 9a.[16] The precursor 5,15-bis(4′-bromophenyl)-10,20-bis(4′-iodophenyl)-porphyrin (*trans*-Br_2I_2TPP) (Figure 9b), equipped with two bromine and two iodine substituents at orthogonal terminal sites, was first coupled into linear chains by thermal activation of the C−I bonds at 393 K on Au(111) (Figure 9c). Subsequently, thermal activation of the C−Br bonds at 523 K resulted in the formation of 2D conjugated networks (Figure 9d). Once the first interchain C−C bond was formed, the activated sites automatically arranged themselves for further C−C bond formation. This "molecular zipper" template effect is possible because all activated sites are equally spaced along each TPP polymer chain. It is therefore reasonable to expect that the 2D networks formed by this hierarchical strategy contain fewer defects than those obtained via one-step growth procedures. A similar approach was also been used by Lin et al.,[46] where linear templates based on pyridyl−Cu−pyridyl coordination effectively triggered Ullmann coupling of the substituted porphyrin monomers on Au(111) into structures with enhanced long-range order. Hierarchical coupling was also performed with 1,3-bis(*para*-bromophenyl)-5-(*para*-iodophenyl)benzene (BIB) (Figure 9e), a molecule with the same carbon skeleton as TBPB in Figure 4a.[14] As shown in Figure 9f, room-temperature deposition of BIB on Au(111) resulted in C−I bond dissociation and formation of 3,3‴,5,5‴-tetra(*para*-bromophenyl)-1,1′:4′,1″:4″,1‴-quaterphenyl (TBQ, see Figure 9f, inset) through direct covalent coupling of BIB monoradicals. By thermal C−Br bond activation at 523 K, the bigger TBQ

DOI: 10.1021/acs.accounts.5b00168
Acc. Chem. Res. 2015, 48, 2484−2494

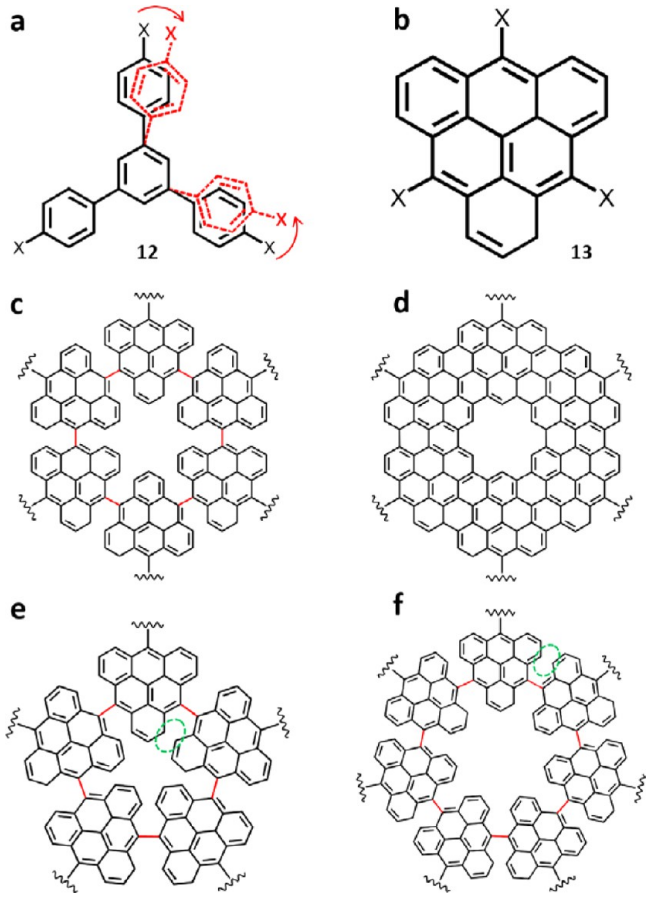

Figure 10. Chemical structures of (a) 1,3,5-tris(4-halophenyl)benzene (**12**, THPB; X represents halogen atoms) and (b) three-fold halogen substituted 1*H*,12d*H*-dibenzo[*cd*,*mn*]pyrene (**13**, THDP). (c, e, f) Structural motifs via C−C coupling of six, five, and seven monomer **13**, respectively. (d) Porous hydrogenated graphene units formed by cyclo-dehydrogenation of structure in panel c.

molecules then coupled into porous covalent networks (Figure 9g) with improved structure quality compared with that obtained through one-step coupling of TBPB (Figure 4a). The hierarchical strategy can be extended by using a broader range of reactive substituents, including different halogens, alkynl, or special C−H bonds, such as in 4Ph obtained through Ullmann coupling of 4-bromobiphenyl (BBP) followed by cross-dehydrogenative coupling into zigzag-shaped polyphenylene chains.[47]

Further challenges arise from C−C linkage in unwanted positions or orientations. As mentioned above, such "wrong" connections stem from the deformation of carbon skeletons of precursor monomers due to thermal agitation under 2D confinement. For example, the frequently used haloarene monomer with 3-fold symmetry in Figure 10a is expected to undergo in-plane deformation on a substrate, with an amplitude depending on temperature. The three equivalent terminal phenyl units (marked in red in Figure 10a) can deviate from their ideal positions (black) through bending of C−C σ bonds between two neighboring phenyl units, reducing the 3-fold molecular symmetry. As a result, various polygons like pentagons and heptagons were observed after C−C coupling, besides hexagons as the ideal structural motif.[35]

To avoid such deformation, precursors should be designed with an enhanced structural rigidity, such as the precursor **13** (THDP, Figure 10b) with a tight triangular pyrene core, which guarantees the 3-fold symmetry of the C−X bonds. The formed C−C σ bonds play another role in the emergence of wrong connections. The ideal structural motif in Figure 10c can be acquired by C−C coupling of six THDP molecules. Further cyclo-dehydrogenation of this structure would lead to porous hydrogenated graphene units as shown in Figure 10d. The structural motifs in Figure 10e,f can be obtained by coupling of five and seven THDPs if the formed C−C σ bonds bend during the coupling. However, the steric repulsion between the C−H bonds (marked in green in Figure 10e,f) of two neighboring THDP units would obviously be increased, compared with the six-membered ring in Figure 10c. It is therefore expected that six-membered rings are favored over the unwanted five- and seven-membered rings. Apparently, with the introduction of steric hindrance between building blocks in the coupling process by employing precursor monomers with high rigidity and appropriately placed halogen substituents, 2D networks with enhanced domain size and structural uniformity may be obtained.

Another potentially adverse steric influence results from halogen byproducts, which usually cannot be removed by thermal desorption. However, dosing H_2 or atomic H to Br/Au(111) surface caused desorption of HBr under mild conditions.[48] Alternatively, it was shown that halogen atoms can be prevented from reaching the substrate by preactivation of the C−X bonds in the evaporator, such as method II for activation of brominated TPP reported previously,[27] where only TPP radicals were evaporated. However, this process may be difficult to control in general.

■ CONCLUSIONS AND OUTLOOK

Various surface-assisted C−C coupling strategies for the fabrication of low-dimensional conjugated nanostructures have been reviewed, including Ullmann coupling or the relatively clean Glaser and dehydrogenative coupling between aromatic building blocks. Advantages and disadvantages of these coupling strategies have been discussed, considering the aim of obtaining large-scale high-quality nanostructures. For Ullmann coupling, steric effects of the chemisorbed halogen byproducts undermine the quality of the networks compared with the "cleaner" coupling strategies. The latter, especially the Glaser and dehydrogenative coupling, however, are plagued by multiple side reaction pathways and low selectivity, respectively. The general challenges for these strategies, including lack of network compactness and structural uniformity, have been emphasized. So far, these issues have not been thoroughly resolved; nevertheless, they can be addressed within certain limits. The network compactness can be improved by adjusting a small relative coupling probability, $p = \nu_{coupl}/(\nu_{coupl} + \nu_{diff})$ factor of the specific precursor/substrate system or by controlling the growth dynamics via a hierarchical coupling strategy. The structural uniformity of the obtained networks can be improved by elimination of precursor monomer deformation and orientational deviations of the formed C−C σ bonds, which requires the design of precursor with more rigid carbon skeleton and placing the reactive groups at suitable positions in the molecule.

Other solutions to these challenges may be developed on the basis of the following considerations. A lower p value requires a larger precursor diffusion rate, ν_{diff}, which can be achieved by employing substrates that interact more weakly with organic molecules than the currently used metal surfaces, for example,

DOI: 10.1021/acs.accounts.5b00168
Acc. Chem. Res. 2015, 48, 2484−2494

nonmetal substrates like HOPG, boron nitride, and silicon. However, these substrates often have low potential for precursor activation. In addition, the intermediate radicals may form covalent bonds to these substrates. A method of preactivating precursors into free radicals before they reach the substrate can be developed to induce the reaction on inert substrates, for example, by passing the evaporated precursors through heated tubes. This method may also provide a feasible route to fabrication of carbon-based nanostructures on arbitrary substrates, which is required for their application in electronic devices.

AUTHOR INFORMATION

Corresponding Author

*E-mail: jfzhu@ustc.edu.cn.

Funding

J.F.Z. acknowledges the financial support from the National Basic Research Program of China (Grant 2013CB834605), the National Natural Science Foundation of China (Grants 21173200 and 21473178), Scientific Research Grant of Hefei Science Center of CAS (SRG-HSC) (Grant 2015SRG-HSC031), and the Specialized Research Fund for the Doctoral Program of Higher Education of Ministry of Education (Grant No. 20113402110029). J.M.G. thanks the Chinese Academy of Sciences for a Visiting Professorship for Senior International Scientists (Grant No. 2011T2J33), and the Deutsche Forschungsgemeinschaft (DFG) for support through the Collaborative Research Center (CRC) 1083.

Notes

The authors declare no competing financial interest.

Biographies

Qitang Fan received his Bachelor of Science in Physics from Nanchang University in 2011 and is currently a Ph.D. candidate at University of Science and Technology of China (USTC). His research interests focus on surface supramolecular assembly and on-surface synthesis of macromolecules.

J. Michael Gottfried is Professor of Physical Chemistry in Marburg/Germany. He studied Chemisty in Darmstadt, St. Andrews, and Berlin and received his Ph.D. in 2003 from the Freie Universität Berlin under the guidance of Klaus Christmann. After postdoctoral research with Charlie Campbell at the University of Washington, he was an assistant of Hans-Peter Steinrück at the Universität Erlangen-Nürnberg. His research focuses on the surface chemistry of reactive molecular model systems.

Junfa Zhu received his Ph.D. in Physical Chemistry from USTC in 1999. After several years working in the Institute of Experimental Physics, Johannes-Kepler-Universität Linz, Austria, Lehrstuhl für Physikalische Chemie II, Friedrich-Alexander-Universität Erlangen-Nürnberg, Germany, and Department of Chemistry, University of Washington, WA, USA, he returned to USTC in December, 2006, and became a professor at National Synchrotron Radiation Laboratory, USTC, under the support of "Hundred Talent Program" of Chinese Academy of Sciences. His research interests mainly focus on in situ studies of surface and interface structures and properties of functional materials using advanced surface science techniques.

REFERENCES

(1) Novoselov, K. S.; Geim, A. K.; Morozov, S. V.; Jiang, D.; Katsnelson, M. I.; Grigorieva, I. V.; Dubonos, S. V.; Firsov, A. A. Two-dimensional gas of massless Dirac fermions in graphene. *Nature* **2005**, *438*, 197−200.

(2) Pedersen, T.; Flindt, C.; Pedersen, J.; Mortensen, N.; Jauho, A.-P.; Pedersen, K. Graphene antidot lattices: designed defects and spin qubits. *Phys. Rev. Lett.* **2008**, *100*, 136804.

(3) Ouyang, F.; Peng, S.; Liu, Z.; Liu, Z. Bandgap opening in graphene antidot lattices: the missing half. *ACS Nano* **2011**, *5*, 4023−4030.

(4) Eroms, J.; Weiss, D. Weak localization and transport gap in graphene antidot lattices. *New J. Phys.* **2009**, *11*, 095021.

(5) Kim, M.; Safron, N. S.; Han, E.; Arnold, M. S.; Gopalan, P. Fabrication and characterization of large-area, semiconducting nanoperforated graphene materials. *Nano Lett.* **2010**, *10*, 1125−1131.

(6) Sinitskii, A.; Tour, J. M. Patterning graphene through the self-assembled templates: toward periodic two-dimensional graphene nanostructures with semiconductor properties. *J. Am. Chem. Soc.* **2010**, *132*, 14730−14732.

(7) Bai, J.; Zhong, X.; Jiang, S.; Huang, Y.; Duan, X. Graphene nanomesh. *Nat. Nanotechnol.* **2010**, *5*, 190−194.

(8) Bieri, M.; Treier, M.; Cai, J.; Ait-Mansour, K.; Ruffieux, P.; Groening, O.; Groening, P.; Kastler, M.; Rieger, R.; Feng, X.; Müllen, K.; Fasel, R. Porous graphenes: two-dimensional polymer synthesis with atomic precision. *Chem. Commun.* **2009**, 6919−6921.

(9) Cai, J.; Ruffieux, P.; Jaafar, R.; Bieri, M.; Braun, T.; Blankenburg, S.; Muoth, M.; Seitsonen, A. P.; Saleh, M.; Feng, X.; Müllen, K.; Fasel, R. Atomically precise bottom-up fabrication of graphene nanoribbons. *Nature* **2010**, *466*, 470−473.

(10) Basagni, A.; Sedona, F.; Pignedoli, C. A.; Cattelan, M.; Nicolas, L.; Casarin, M.; Sambi, M. Molecules−oligomers−nanowires−graphene nanoribbons: a bottom-up stepwise on-surface covalent synthesis preserving long-range order. *J. Am. Chem. Soc.* **2015**, *137*, 1802−1808.

(11) Zhang, H.; Lin, H.; Sun, K.; Chen, L.; Zagranyarski, Y.; Aghdassi, N.; Duhm, S.; Li, Q.; Zhong, D.; Li, Y.; Müllen, K.; Fuchs, H.; Chi, L. On-surface synthesis of rylene-type graphene nanoribbons. *J. Am. Chem. Soc.* **2015**, *137*, 4022−4025.

(12) Treier, M.; Pignedoli, C. A.; Laino, T.; Rieger, R.; Müllen, K.; Passerone, D.; Fasel, R. Surface-assisted cyclodehydrogenation provides a synthetic route towards easily processable and chemically tailored nanographenes. *Nat. Chem.* **2011**, *3*, 61−67.

(13) Wang, W. H.; Shi, X. Q.; Wang, S. Y.; Van Hove, M. A.; Lin, N. Single-molecule resolution of an organometallic intermediate in a surface-supported Ullmann coupling reaction. *J. Am. Chem. Soc.* **2011**, *133*, 13264−13267.

(14) Eichhorn, J.; Nieckarz, D.; Ochs, O.; Samanta, D.; Schmittel, M.; Szabelski, P. J.; Lackinger, M. On-surface Ullmann coupling: the influence of kinetic reaction parameters on the morphology and quality of covalent networks. *ACS Nano* **2014**, *8*, 7880−7889.

(15) Bieri, M.; Nguyen, M. T.; Groning, O.; Cai, J. M.; Treier, M.; Ait-Mansour, K.; Ruffieux, P.; Pignedoli, C. A.; Passerone, D.; Kastler, M.; Müllen, K.; Fasel, R. Two-dimensional polymer formation on surfaces: Insight into the roles of precursor mobility and reactivity. *J. Am. Chem. Soc.* **2010**, *132*, 16669−16676.

(16) Lafferentz, L.; Eberhardt, V.; Dri, C.; Africh, C.; Comelli, G.; Esch, F.; Hecht, S.; Grill, L. Controlling on-surface polymerization by hierarchical and substrate-directed growth. *Nat. Chem.* **2012**, *4*, 215−220.

(17) Fan, Q.; Wang, C.; Liu, L.; Han, Y.; Zhao, J.; Zhu, J.; Kuttner, J.; Hilt, G.; Gottfried, J. M. Covalent, organometallic, and halogen-bonded nanomeshes from tetrabromo-terphenyl by surface-assisted synthesis on Cu(111). *J. Phys. Chem. C* **2014**, *118*, 13018−13025.

(18) Gao, H. Y.; Wagner, H.; Zhong, D.; Franke, J. H.; Studer, A.; Fuchs, H. Glaser coupling at metal surfaces. *Angew. Chem., Int. Ed.* **2013**, *52*, 4024−4028.

(19) Sun, Q.; Zhang, C.; Li, Z.; Kong, H.; Tan, Q.; Hu, A.; Xu, W. On-surface formation of one-dimensional polyphenylene through Bergman cyclization. *J. Am. Chem. Soc.* **2013**, *135*, 8448−8451.

(20) Han, P.; Akagi, K.; Federici Canova, F.; Mutoh, H.; Shiraki, S.; Iwaya, K.; Weiss, P. S.; Asao, N.; Hitosugi, T. Bottom-up graphene-

DOI: 10.1021/acs.accounts.5b00168
Acc. Chem. Res. 2015, 48, 2484−2494

nanoribbon fabrication reveals chiral edges and enantioselectivity. *ACS Nano* **2014**, *8*, 9181−9187.
(21) Sun, Q.; Cai, L.; Ding, Y.; Xie, L.; Zhang, C.; Tan, Q.; Xu, W. Dehydrogenative homocoupling of terminal alkenes on copper surfaces: a route to dienes. *Angew. Chem., Int. Ed.* **2015**, *54*, 4549−4552.
(22) Sun, Q.; Zhang, C.; Kong, H.; Tan, Q.; Xu, W. On-surface aryl-aryl coupling *via* selective C-H activation. *Chem. Commun.* **2014**, *50*, 11825−11828.
(23) Ullmann, F.; Bielecki, J. Synthesis in the Biphenyl Series. J. *Ber. Dtsch. Chem. Ges.* **1901**, *34*, 2174−2185.
(24) Xi, M.; Bent, B. E. Mechanisms of the Ullmann coupling reaction in adsorbed monolayers. *J. Am. Chem. Soc.* **1993**, *115*, 7426−7433.
(25) Lewis, E. A.; Murphy, C. J.; Liriano, M. L.; Sykes, E. C. Atomic-scale insight into the formation, mobility and reaction of Ullmann coupling intermediates. *Chem. Commun.* **2014**, *50*, 1006−1008.
(26) Lewis, E. A.; Murphy, C. J.; Pronschinske, A.; Liriano, M. L.; Sykes, E. C. Nanoscale insight into C-C coupling on cobalt nanoparticles. *Chem. Commun.* **2014**, *50*, 10035−10037.
(27) Grill, L.; Dyer, M.; Lafferentz, L.; Persson, M.; Peters, M. V.; Hecht, S. Nano-architectures by covalent assembly of molecular building blocks. *Nat. Nanotechnol.* **2007**, *2*, 687−691.
(28) Cai, J.; Pignedoli, C. A.; Talirz, L.; Ruffieux, P.; Sode, H.; Liang, L.; Meunier, V.; Berger, R.; Li, R.; Feng, X.; Müllen, K.; Fasel, R. Graphene nanoribbon heterojunctions. *Nat. Nanotechnol.* **2014**, *9*, 896−900.
(29) Lipton-Duffin, J. A.; Ivasenko, O.; Perepichka, D. F.; Rosei, F. Synthesis of polyphenylene molecular wires by surface-confined polymerization. *Small* **2009**, *5*, 592−597.
(30) Lipton-Duffin, J. A.; Miwa, J. A.; Kondratenko, M.; Cicoira, F.; Sumpter, B. G.; Meunier, V.; Perepichka, D. F.; Rosei, F. Step-by-step growth of epitaxially aligned polythiophene by surface-confined reaction. *Proc. Natl. Acad. Sci. U. S. A.* **2010**, *107*, 11200−11204.
(31) Fan, Q.; Wang, C.; Han, Y.; Zhu, J.; Hieringer, W.; Kuttner, J.; Hilt, G.; Gottfried, J. M. Surface-assisted organic synthesis of hyperbenzene nanotroughs. *Angew. Chem., Int. Ed.* **2013**, *52*, 4668−4672.
(32) Fan, Q.; Wang, C.; Han, Y.; Zhu, J.; Kuttner, J.; Hilt, G.; Gottfried, J. M. Surface-assisted formation, assembly, and dynamics of planar organometallic macrocycles and zigzag shaped polymer chains with C-Cu-C bonds. *ACS Nano* **2014**, *8*, 709−718.
(33) Park, J.; Kim, K. Y.; Chung, K.-H.; Yoon, J. K.; Kim, H.; Han, S.; Kahng, S.-J. Interchain interactions mediated by br adsorbates in arrays of metal-organic hybrid chains on Ag(111). *J. Phys. Chem. C* **2011**, *115*, 14834−14838.
(34) Di Giovannantonio, M.; El Garah, M.; Lipton-Duffin, J.; Meunier, V.; Cardenas, L.; Fagot Revurat, Y.; Cossaro, A.; Verdini, A.; Perepichka, D. F.; Rosei, F.; Contini, G. Insight into organometallic intermediate and its evolution to covalent bonding in surface-confined Ullmann polymerization. *ACS Nano* **2013**, *7*, 8190−8198.
(35) Blunt, M. O.; Russell, J. C.; Champness, N. R.; Beton, P. H. Templating molecular adsorption using a covalent organic framework. *Chem. Commun.* **2010**, *46*, 7157−7159.
(36) Faury, T.; Clair, S.; Abel, M.; Dumur, F.; Gigmes, D.; Porte, L. Sequential linking to control growth of a surface covalent organic framework. *J. Phys. Chem. C* **2012**, *116*, 4819−4823.
(37) Fan, Q.; Wang, T.; Liu, L.; Zhao, J.; Zhu, J.; Gottfried, J. M. Tribromobenzene on Cu(111): Temperature-dependent formation of halogen-bonded, organometallic, and covalent nanostructures. *J. Chem. Phys.* **2015**, *142*, 101906.
(38) Chen, M.; Xiao, J.; Steinrück, H.-P.; Wang, S.; Wang, W.; Lin, N.; Hieringer, W.; Gottfried, J. M. Combined photoemission and scanning tunneling microscopy study of the surface-assisted Ullmann coupling reaction. *J. Phys. Chem. C* **2014**, *118*, 6820−6830.
(39) Zhou, H.; Liu, J.; Du, S.; Zhang, L.; Li, G.; Zhang, Y.; Tang, B. Z.; Gao, H. J. Direct visualization of surface-assisted two-dimensional diyne polycyclotrimerization. *J. Am. Chem. Soc.* **2014**, *136*, 5567−5570.
(40) Liu, J.; Ruffieux, P.; Feng, X.; Müllen, K.; Fasel, R. Cyclotrimerization of arylalkynes on Au(111). *Chem. Commun.* **2014**, *50*, 11200−11203.
(41) Zhang, Y. Q.; Kepcija, N.; Kleinschrodt, M.; Diller, K.; Fischer, S.; Papageorgiou, A. C.; Allegretti, F.; Björk, J.; Klyatskaya, S.; Klappenberger, F.; Ruben, M.; Barth, J. V. Homo-coupling of terminal alkynes on a noble metal surface. *Nat. Commun.* **2012**, *3*, 1286.
(42) Cirera, B.; Zhang, Y. Q.; Björk, J.; Klyatskaya, S.; Chen, Z.; Ruben, M.; Barth, J. V.; Klappenberger, F. Synthesis of extended graphdiyne wires by vicinal surface templating. *Nano Lett.* **2014**, *14*, 1891−1897.
(43) Zhong, D.; Franke, J. H.; Podiyanachari, S. K.; Blomker, T.; Zhang, H.; Kehr, G.; Erker, G.; Fuchs, H.; Chi, L. Linear alkane polymerization on a gold surface. *Science* **2011**, *334*, 213−216.
(44) Sun, Q.; Zhang, C.; Cai, L.; Xie, L.; Tan, Q.; Xu, W. On-surface formation of two-dimensional polymer *via* direct C-H activation of metal phthalocyanine. *Chem. Commun.* **2015**, *51*, 2836−2839.
(45) Wiengarten, A.; Seufert, K.; Auwärter, W.; Ecija, D.; Diller, K.; Allegretti, F.; Bischoff, F.; Fischer, S.; Duncan, D. A.; Papageorgiou, A. C.; Klappenberger, F.; Acres, R. G.; Ngo, T. H.; Barth, J. V. Surface-assisted dehydrogenative homocoupling of porphine molecules. *J. Am. Chem. Soc.* **2014**, *136*, 9346−9354.
(46) Lin, T.; Shang, X. S.; Adisoejoso, J.; Liu, P. N.; Lin, N. Steering on-surface polymerization with metal-directed template. *J. Am. Chem. Soc.* **2013**, *135*, 3576−3582.
(47) Zhang, C.; Sun, Q.; Chen, H.; Tan, Q.; Xu, W. Formation of polyphenyl chains through hierarchical reactions: Ullmann coupling followed by cross-dehydrogenative coupling. *Chem. Commun.* **2015**, *51*, 495−498.
(48) Bronner, C.; Björk, J.; Tegeder, P. Tracking and removing Br during the on-surface synthesis of a graphene nanoribbon. *J. Phys. Chem. C* **2015**, *119*, 486−493.

DOI: 10.1021/acs.accounts.5b00168
Acc. Chem. Res. 2015, 48, 2484−2494